ELECTRONIC SUPPORTING INFORMATION

Aqua and ammine 3d metal complexes with anion-radical of difurazanopyrazine

Sergey Fokin,✉ Svyatoslav Tolstikov, Vitaly Morozov, Arkady Samsonenko, Galina Romanenko, ✉ Artem Bogomyakov

International Tomography Center SB RAS, Novosibirsk, Russia

✉ *E-mail:* fokin@tomo.nsc.ru, romanenko@tomo.nsc.ru

CONTENT

1. IR spectroscopy

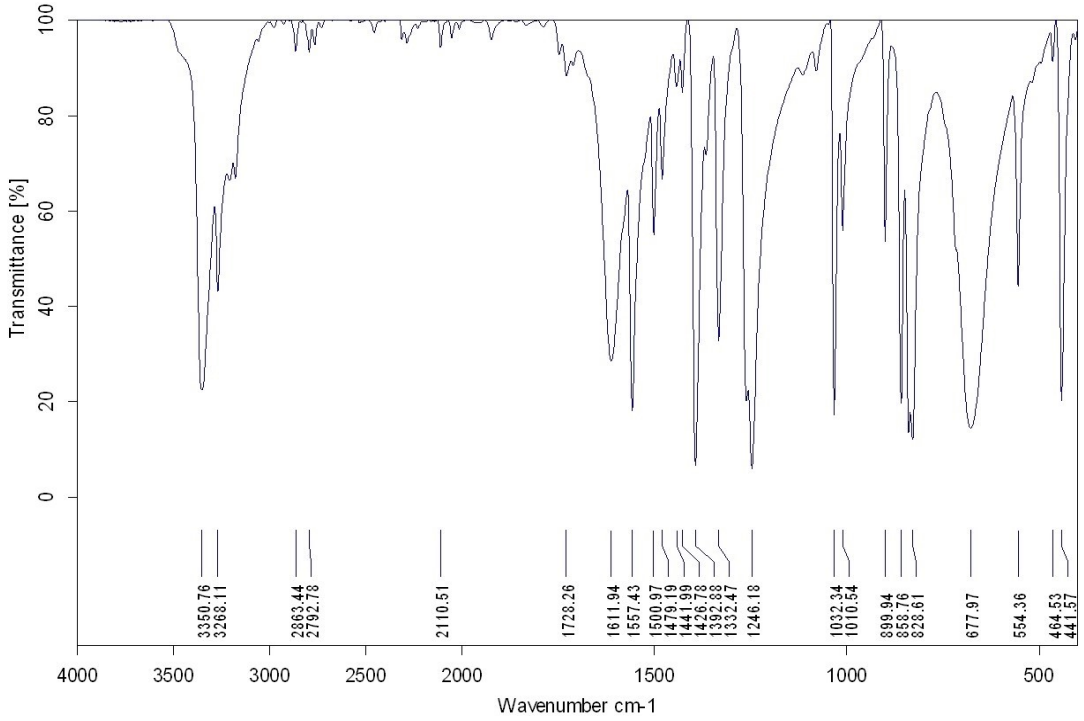

Fig. S1. IR spectrum of solid $[CuL_2(NH_3)_4]$

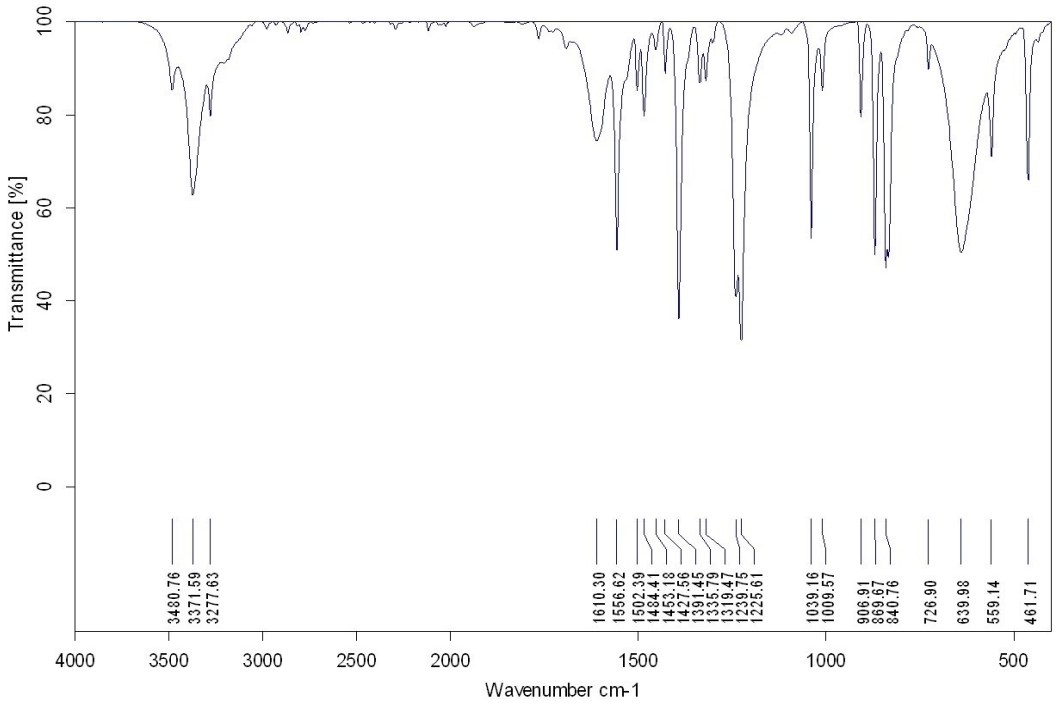

Fig. S2. IR spectrum of solid $[NiL_2(NH_3)_4]$

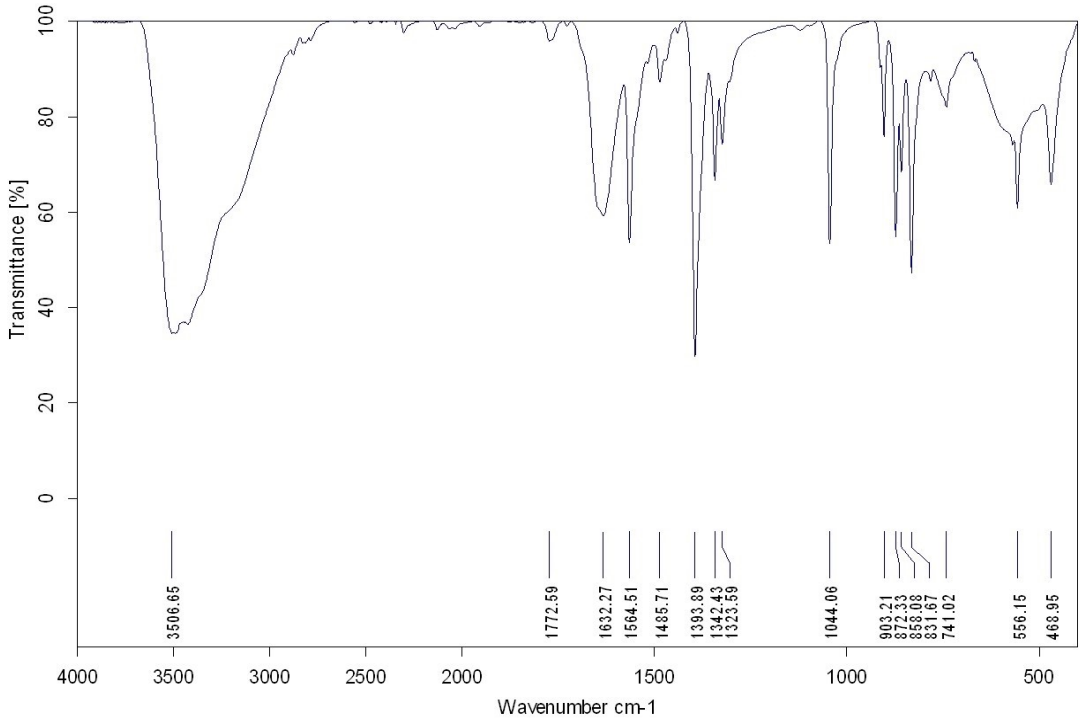

Fig. S3. IR spectrum of solid $[NiL_2(H_2O)_4]\cdot 2H_2O$

2. Crystal data and details of SC XRD experiments

Table S1. Crystal data and details of SC XRD experiments

Formula	$[NiL_2(NH_3)_4]$	$[CuL_2(NH_3)_4]$	$[NiL_2(H_2O)_4]\cdot 2H_2O$	$[CoL_2(H_2O)_4]\cdot 2H_2O$
FW	455.05	459.88	495.01	495.23
T, K	296	296	296	296
Space group, Z	$P2_1/n$, 2	$P2_1/n$, 2	$P2_1/n$, 2	$P2_1/n$, 2
a,	8.3767(3)	8.3743(3)	9.2553(5)	9.2929(7)
b,	11.2253(4)	10.4991(4)	6.5752(4)	6.5584(4)
c, Å	9.2089(3)	9.5646(4)	14.3428(7)	14.4252(8)
β, °	111.9995(14)	108.1066(18)	95.900(4)	95.720(4)
V, Å^3	802.87(5)	799.30(5)	868.21(8)	874.79(10)
D_{calc}, g/cm^3	1.882	1.911	1.893	1.880
θ_{max}, °	67.864	67.556	28.147	31.729
I_{hkl} total/uniq	5683 / 1437	7965 / 1439	8447 / 2138	2753 / 2753
R_{int}	0.0241	0.0306	0.0791	0.0653
I_{hkl} uniq ($I>2\sigma_I$) / N	1333 / 158	1362 / 157	1457 / 169	1775 / 167
Goof	1.073	1.048	0.966	0.923
$R1$ / $wR2$ ($I>2\sigma_I$)	0.0291 / 0.0821	0.0296 / 0.0826	0.0565 / 0.1646	0.0475 / 0.1046
$R1$ / $wR2$ (all data)	0.0310 / 0.0841	0.0309 / 0.0842	0.0810 / 0.1806	0.0751 / 0.1144
CCDC	2408083	2408084	2408085	2408082

Table S2. Short contacts and H-bonds in studied compounds

Contact	$[NiL_2(NH_3)_4]$	$[CuL_2(NH_3)_4]$	$[NiL_2(H_2O)_4]\cdot 2H_2O$	$[CoL_2(H_2O)_4]\cdot 2H_2O$
$O_L\ldots O_L$	3.256 3.126	3.294 3.303	2.636	2.659
$O_L\ldots N_L$	3.093 3.150	3.199 3.295	–	–
C…C / C…N / N…N	3.330–3.444	3.276 3.170 3.294	3.277–3.436	3.253–3.434
Ow-H…Ow	–	–	2.727, 3.043	2.722, 3.033
$N\text{-}H\ldots O_L/N_L$	3.381, 3.386	3.185	–	–
$N\text{-}H\ldots O_L$	3.404	3.048	–	–
$Ow\text{-}H\ldots N_L$	–	–	2.966, 2.962 2.979, 3.078	2.965, 2.962 2.846, 3.078

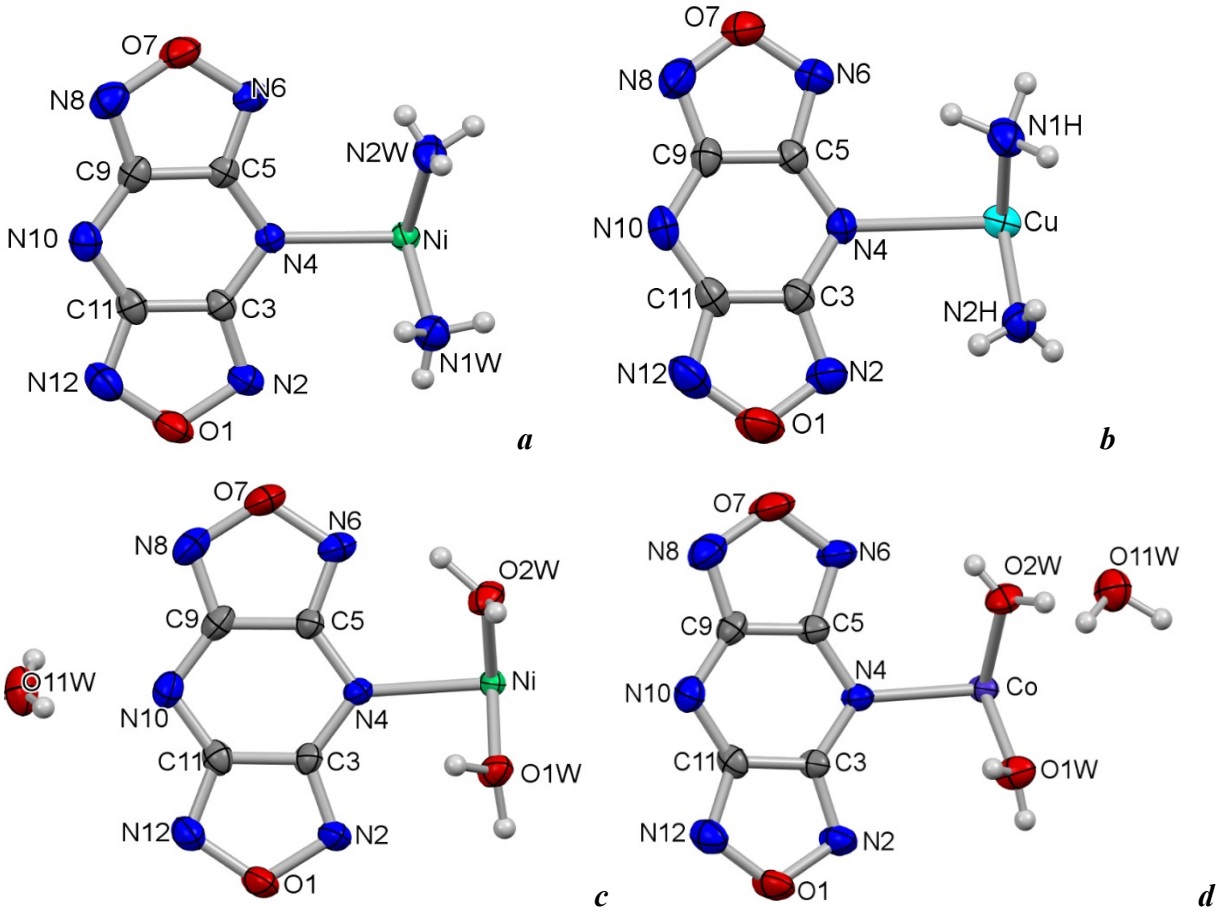

Fig. S4. Independent parts of crystal structures $[NiL_2(NH_3)_4]$ (*a*), $[CuL_2(NH_3)_4]$ (*b*), $[NiL_2(H_2O)_4]\cdot 2H_2O$ (*c*), $[CoL_2(H_2O)_4]\cdot 2H_2O$ (*d*).

3. Powder XRD

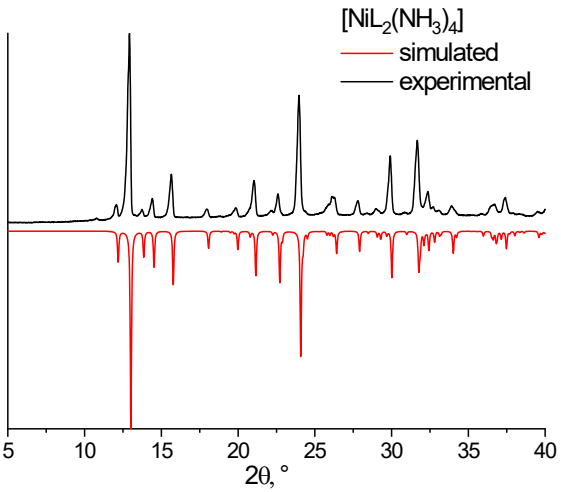

Figure S5. Powder XRD data for $[NiL_2(NH_3)_4]$.

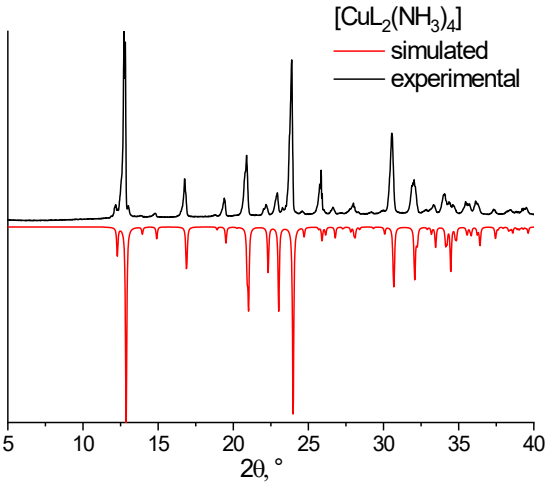

Figure S6. Powder XRD data for $[CuL_2(NH_3)_4]$.

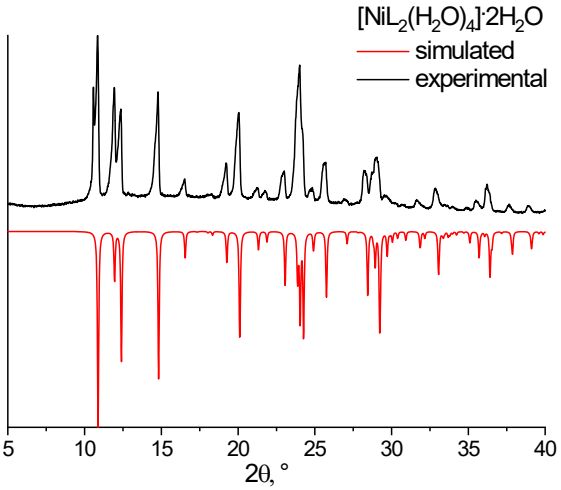

Figure S7. Powder XRD data for $[NiL_2(H_2O)_4]\cdot 2H_2O$

4. Details of quantum-chemical calculations

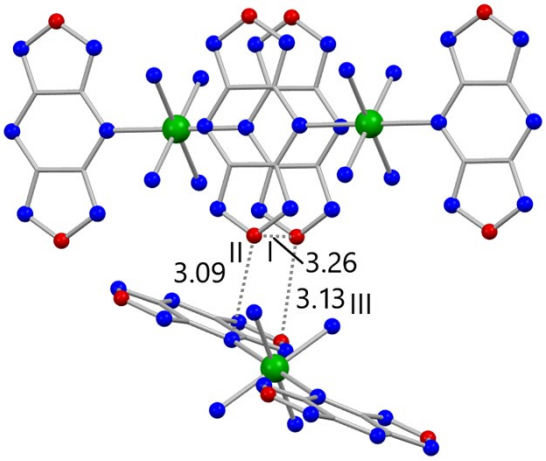

Fig. S8. Pairs of radical anions L in the $[NiL_2(NH_3)_4]$ structure selected for quantum chemical calculations.

Table S3. Exchange integrals (J, cm^{-1}) inside the complex and various pairs of radical anions L for $[NiL_2(NH_3)_4]$ and $[CuL_2(NH_3)_4]$ (Fig. S8)

Complex	$[NiL_2(NH_3)_4]$				$[CuL_2(NH_3)_4]$			
DFT level	**Ni–L**	**I***	**II****	**III****	**Cu–L**	**I***	**II****	**III****
B3LYP/ def2-tzvpp	38.6	-624	2.9	-9.2	0.8	-460	-5.1	-0.52
TPSSh/ def2-tzvpp	42.8	-670	2.5	-10.6	-0.42	-500	-6.1	-1.0
cam-B3LYP/ def2-tzvpp	31.0	-464	2.9	-6.2	0.61	-340	-3.6	0.13
lc-BLYP/ def2-tzvpp	36.4	-440	2.8	-5.9	0.87	-321	-3.5	0.42
wB97-mv/ def2-tzvpp	19.5	-455	2.8	-5.9	0.97	-336	-3.7	0.3

* – L···L pairs along chains of spin triads L-Ni-L

** – L···L pairs belonging to neighboring chains of spin triads L-Ni-L

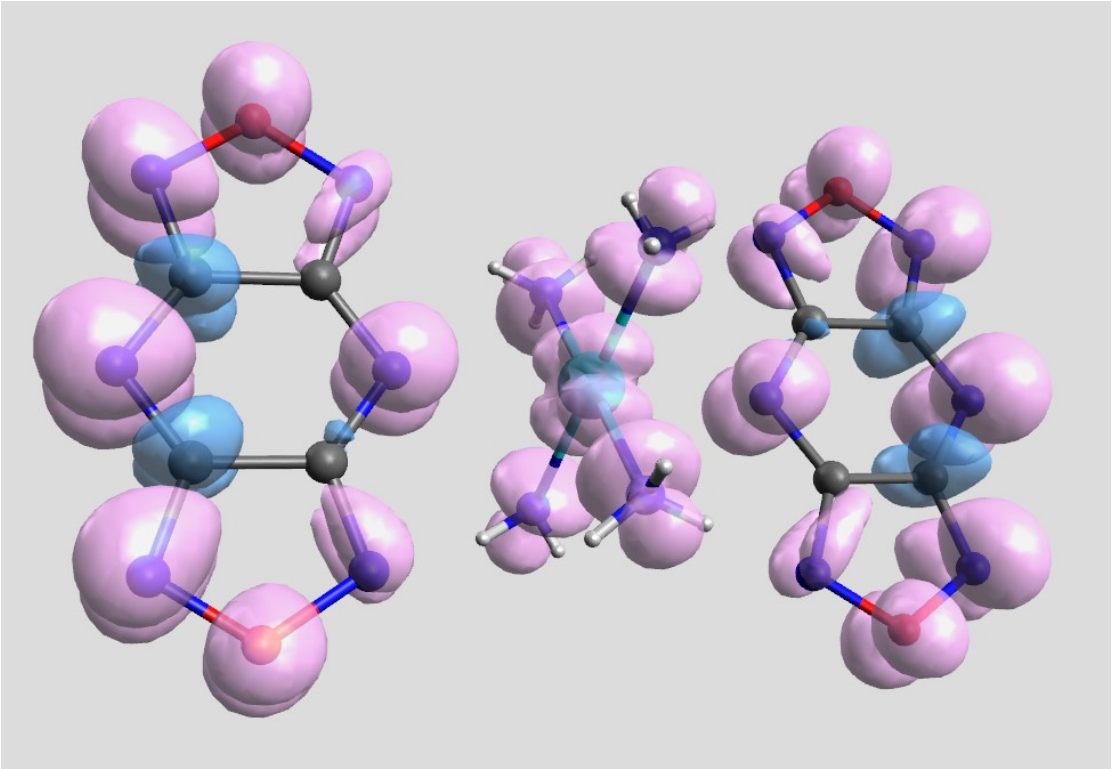

Fig. S9. Spin density distribution (ρ = 0.002) in $[CuL_2(NH_3)_4]$ molecule. TPSSh/def2-TZVP level of DFT. Pink color corresponds to positive sign of spin density, blue color – to negative sign.

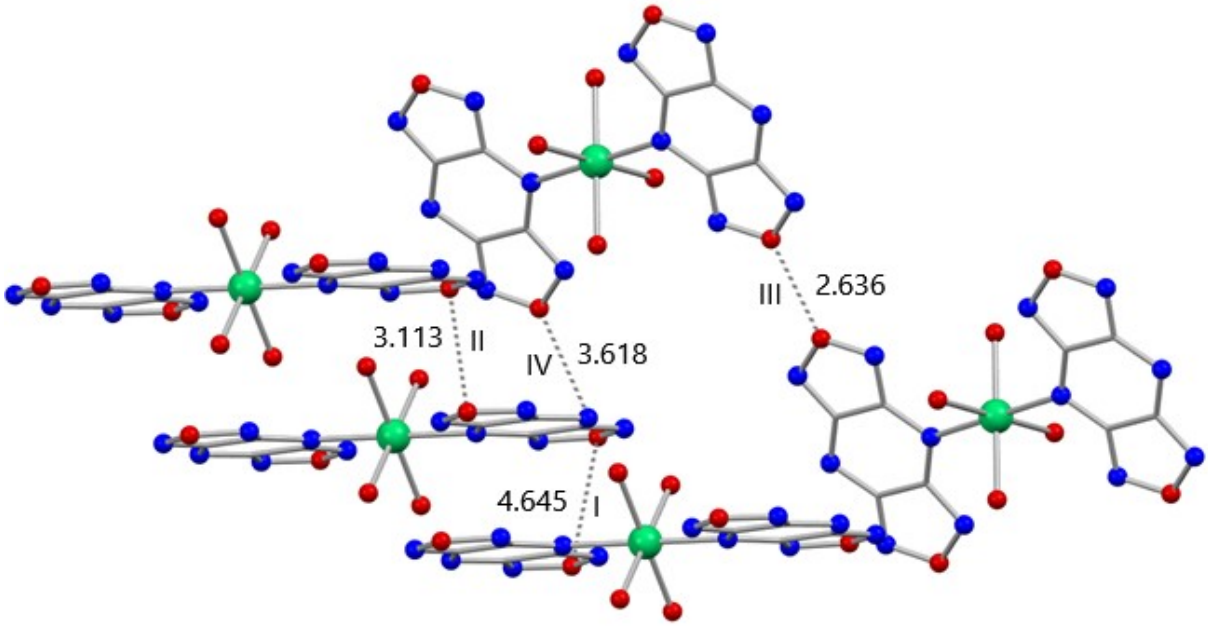

Fig. S10. Pairs of radical anions L in the $[NiL_2(H_2O)_4]\cdot 2H_2O$ structure selected for quantum chemical calculations (the $O_F\cdots O_F$ distances between the O atoms of the furazan rings are shown).

Table S4. DFT calculated intramolecular J_{M-L} exchange integral and intermolecular J_{L-L} exchange integrals for various pairs of radical-anions L in solid $[NiL_2(H_2O)_4]\cdot 2H_2O$ (Figure S10)

	J_{Ni-L}, cm^{-1}	J_{L-L}, cm^{-1}			
DFT level		**I***	**II****	**III****	**IV****
$O_F \ldots O_F$, Å		4.645	3.113	2.636	3.618
B3LYP/ def2-tzvpp	38.4	15.6	-6.5	-2.8	5.4
TPSSh/ def2-tzvpp	42.2	12.3	-9.6	-3.4	4.6
cam-B3LYP/ def2-tzvpp	31.1	23.9	-2.0	-1.8	6.4
lc-BLYP/ def2-tzvpp	36.2	25.8	-2.8	-1.9	6.6
wB97-mv/ def2-tzvpp	26.3	26.8	-2.2	-1.7	6.3

* – L···L pairs along chains of spin triads L-Ni-L

** – L···L pairs belonging to neighboring chains of spin triads L-Ni-L

5. EPR spectroscopy study

4.1. EPR spectroscopy of powder samples $[ML_2(NH_3)_4]$.

Powder samples of $[ML_2(NH_3)_4]$ were prepared by grinding crystals of complexes with KBr in a 1:10 mass ratio. Continuous-wave (CW) X-band (~9.7 GHz) electron paramagnetic resonance (EPR) spectra of powder samples were recorded within the temperature range of 25–285 K using a Bruker Elexsys E580 spectrometer equipped with an Oxford Instruments temperature control system. Measurements were conducted at a microwave power of ~ 0.2 mW with a modulation amplitude of 0.1 mT at 100 kHz. EPR data were simulated using EasySpin toolbox.[1] No EPR signals for the powder sample of the $[NiL_2(NH_3)_4]$ complex were detected in the temperature range of 25–300 K, most likely due to the non-Kramers nature of the Ni(II) ion and the resulting zero-field splitting of the triplet ground state.

EPR spectra of $[CuL_2(NH_3)_4]$ in the temperature range of 25–300 K are shown in Figure S8. The EPR spectra were analyzed within an effective spin model (S = 1/2) assuming an axial g tensor (Fig. S8, black lines). At low temperatures (25-150 K), the spectra can be simulated using an axial g-tensor with characteristic principal values $g_\perp$=2.25 and $g_\parallel$=2.06. Above 150 K, both $g_\perp$ and $g_\parallel$ gradually decrease, reaching approximately 2.20 and 2.05 at 285 K, respectively (Fig. S9). The observed decrease in the g-tensor components with increasing temperature can be attributed to the thermally activated weakening of antiferromagnetic coupling between the paramagnetic ligands of neighboring molecules. Upon cooling to 25 K, the contribution of the anion radical spins diminishes due to partial spin compensation arising from strong intermolecular exchange interactions between them.[2] A similar temperature-dependent evolution of the EPR spectrum was previously observed for Cu(II) molecular complexes containing nitroxide radicals, leading to

nearly a twofold change in g-tensor anisotropy between the low- and high-temperature regions.[3]. Thus, the observed variation in the components of the effective g tensor indicates the radical nature of the ligands and confirms the presence of exchange interactions between the anion-radicals and the Cu(II) ion.

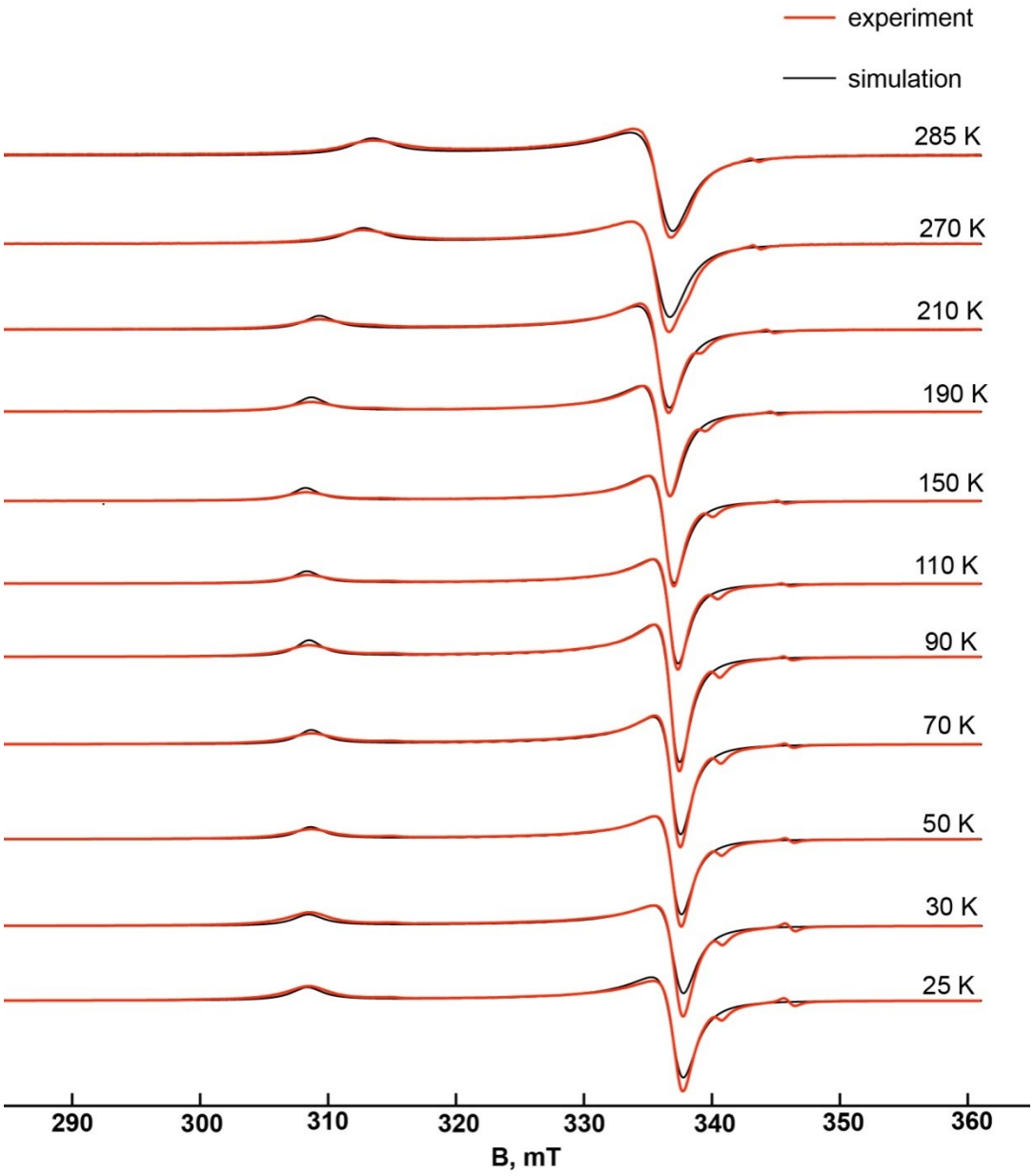

Fig. S11. Normalized EPR spectra of $[CuL_2(NH_3)_4]$ measured in the X-band range over the temperature range of 25 – 285 K.

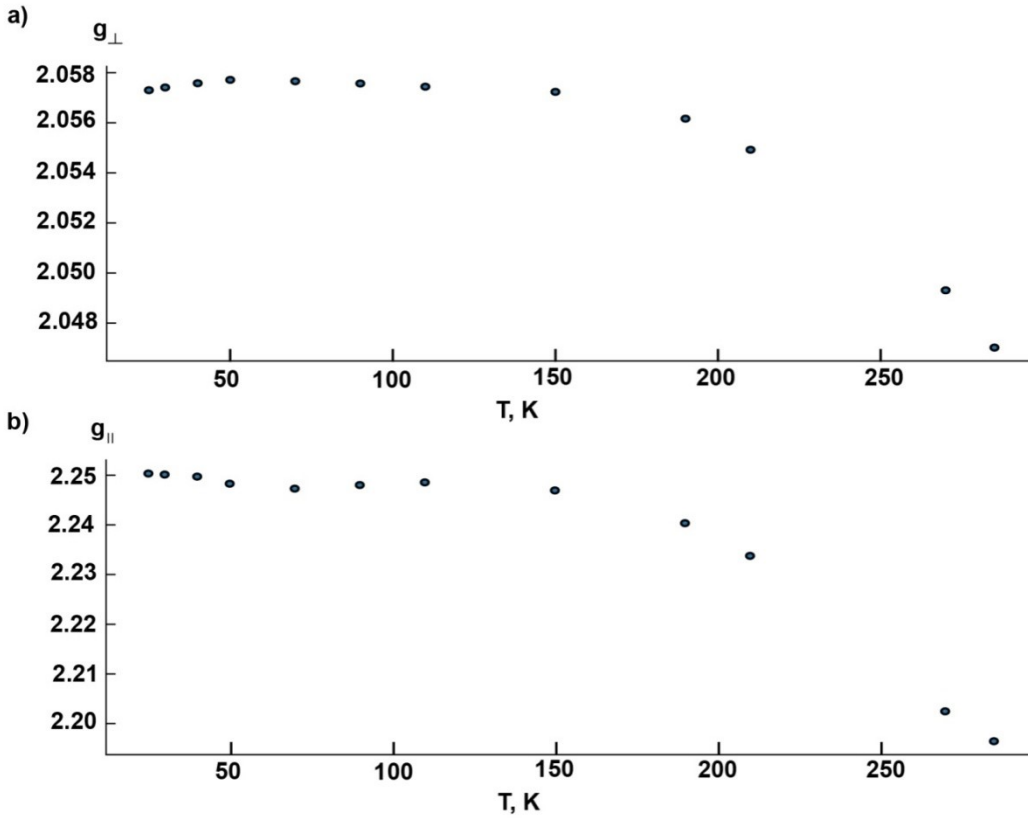

Fig. S12. Temperature dependence of g⊥ (a) and g‖ (b) of the effective g tensor for $[CuL_2(NH_3)_4]$.

5.2. EPR spectroscopy study of $[ML_2(NH_3)_4]$ complexes in solution

CW X-band EPR spectra of the samples dissolved in ethanol were recorded using a Bruker EMX spectrometer at ~9.6 GHz. Spectra were obtained at a microwave power of ~7.95 mW, a modulation amplitude of 0.01 mT at 100 kHz, and a temperature of 25 °C. Analysis of EPR spectra of solutions was performed within the isotropic regime. EPR data were simulated using EasySpin toolbox [1].

EPR spectra of $[CuL_2(NH_3)_4]$ and $[NiL_2(NH_3)_4]$ complexes in ethanol (concentration ~ 1×10^{-4} M) are shown in Figure S13. EPR spectrum of solution in ethanol of paramagnetic salt NaL with diamagnetic cation is also shown in Figure S13. NaL was used as a referenced sample in which only anion-radical is paramagnetic.

All spectra were modeled using a spin S = 1/2 system with an isotropic g factor, coupled to six nitrogen atoms through isotropic hyperfine interactions. Based on the molecular structure of the anion-radical L (Scheme 1), the nitrogen atoms were grouped into two equivalent sets: four equivalent nitrogen atoms with the same hyperfine coupling constant (A_{N1}) and two equivalent nitrogen atoms with coupling constant (A_{N2}). The best-fit values of hyperfine coupling constant parameters are the same for both complexes: A_{N1} = 4.2 MHz and A_{N2} = 12.1 MHz. The best fit g factor values are 2.006 and 2.005 for $[CuL_2(NH_3)_4]$ and $[NiL_2(NH_3)_4]$ samples, respectively. The obtained g-factor values are characteristic of organic radicals.

The EPR spectra of $[CuL_2(NH_3)_4]$ and $[NiL_2(NH_3)_4]$ solutions are similar to the spectrum of the referenced NaL sample solution. The best fit parameters for referenced sample with diamagnetic cation (A_{N1} = 4.2 MHz, A_{N2} = 12.1 MHz, g = 2.002) closely match those of the complexes, confirming that all solution spectra arise from the same radical species. The slight deviations in the g-factor (on the order of 10^{-3}) are attributed to minor magnetic field calibration inaccuracies. These results indicate complex dissociation in solution, yielding spectra corresponding to the non-coordinated anion radical L. The absence of an observable EPR signal of Cu(II) ion in the ethanol solution of $[CuL_2(NH_3)_4]$ may be due to a significant line broadening,[4] caused by the large anisotropy of the g-tensor and hyperfine coupling of Cu(II) ion.

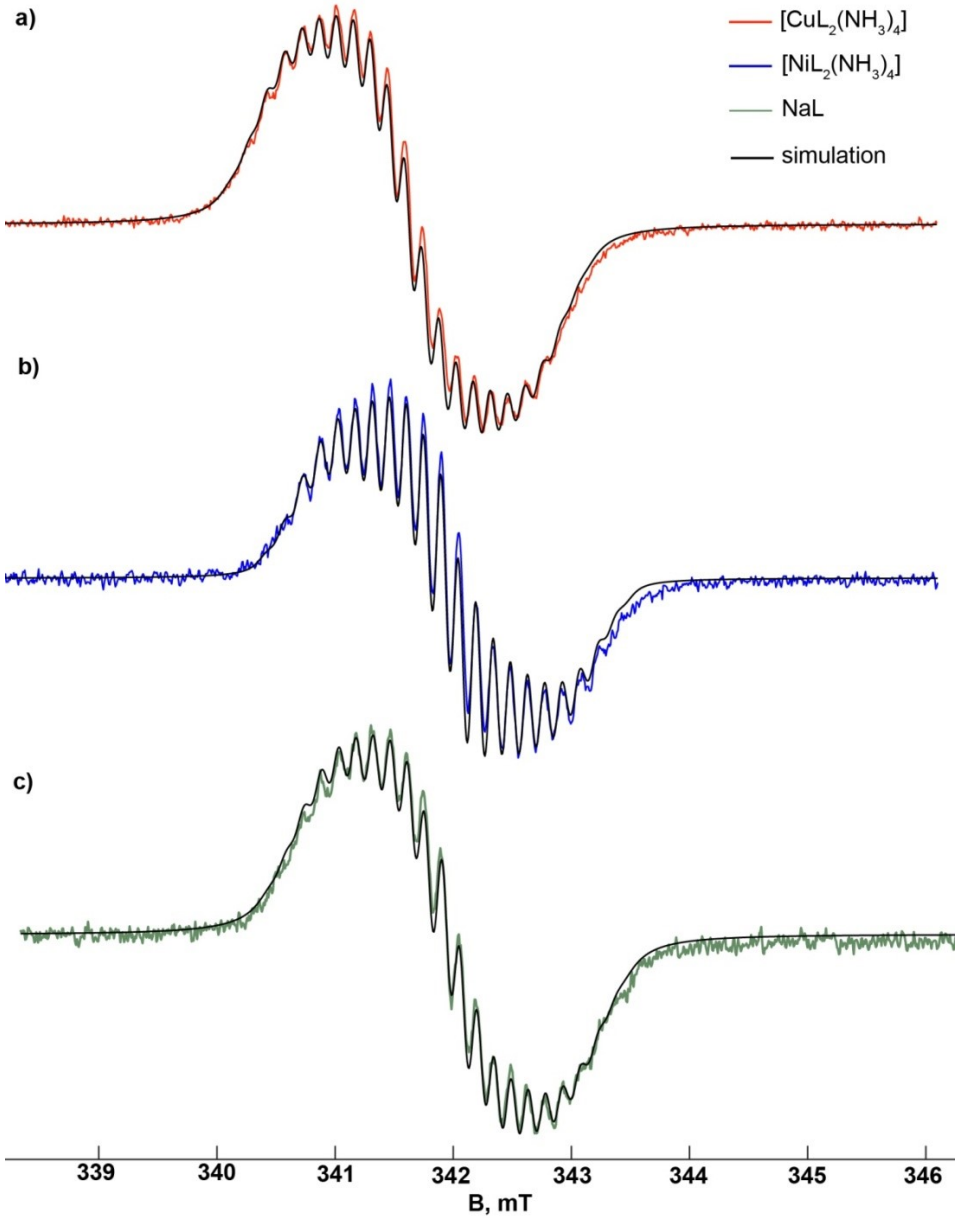

Fig. S13. EPR spectra of $[CuL_2(NH_3)_4]$ (a), $[NiL_2(NH_3)_4]$ (b), and NaL (c) in ethanol solution (concentration ≈ 1×10^{-4} M) at 25 °C.

6. References

1 S. Stoll and A. Schweiger, *J. Magn. Reson.*, 2006, **178**, 42–55.

2 R. Z. Sagdeev, S. E. Tolstikov, S. V. Fokin, I. V. Obsharova, S. V. Tumanov, S. L. Veber, G. V. Romanenko, A. S. Bogomyakov, M. V. Fedin, E. V. Tretyakov, M. Halcrow and V. I. Ovcharenko, *Russ. Chem. Bull.*, 2017, **66**, 222–230.

3 O. N. Chupakhin, E. V. Tretyakov, I. A. Utepova, M. V. Varaksin, G. V. Romanenko, A. S. Bogomyakov, S. L. Veber and V. I. Ovcharenko, *Polyhedron*, 2011, **30**, 647–653.

4 N. P. Kirpichnikova and R. M. Nalbandyan, *Bull. Acad. Sci. USSR Div. Chem. Sci.*, 1970, **19**, 1873–1877.